MDPI

Article

Enzymatic-Induced Calcite Precipitation (EICP) Method for Improving Hydraulic Erosion Resistance of Surface Sand Layer: A Laboratory Investigation

Seyed Mohammad Ali Zomorodian [1,*] , Sodabeh Nikbakht [1], Hamideh Ghaffari [1] and Brendan C. O'Kelly [2,*]

[1] Department of Water Engineering, Shiraz University, Shiraz 7144165186, Iran
[2] Department of Civil, Structural and Environmental Engineering, Trinity College Dublin, D02 PN40 Dublin, Ireland
* Correspondence: mzomorod@shirazu.ac.ir (S.M.A.Z.); bokelly@tcd.ie (B.C.O.)

Abstract: As a bio-inspired calcite precipitation method, bio-grouting via enzymatic-induced calcite precipitation (EICP) uses free urease enzyme to catalyze the urea hydrolysis reaction. This soil stabilization approach is relatively new and insufficiently investigated, especially for applications involving surface layer stabilization of sandy soil deposits for increasing hydraulic erosion resistance. This paper presents a laboratory investigation on the surface erosion resistance improvements for compacted medium-gradation quartz sand specimens mediated using 10 different EICP treatment protocols. They involved single- and two-cycle injections of the urease enzyme (activity of 2400 U/L) and 0.5, 0.75, or 1.0-M urea–$CaCl_2$ cementation solution reagents. The urease enzyme was extracted from watermelon seeds. Erosion rates were determined for various hydraulic shear stresses applied using the erosion function apparatus. The spatial distribution and morphology of precipitated calcite within the pore-void spaces of the crustal sand layer were investigated with a scanning electron microscope. Compared to untreated sand, all 10 investigated EICP treatment protocols produced substantially improved erosion resistance, especially for the higher cementation solution concentration (1.0 M). Of these 10 EICP protocols, a single cycle of enzyme–1.0-M-cementation solutions injections was identified as the more pragmatic option for achieving near-optimum erosion resistance improvements. Highest and lowest amounts (18.8 and 5.0 wt%) of precipitated calcite corresponded to the best and worst performing EICP-treated specimens, although the calcite's spatial distribution in treated specimens is another important factor.

Keywords: bio-cementation; bio-grouting; erosion function apparatus; hydraulic erosion; scouring; soil stabilization

1. Introduction

The geotechnical engineering sector uses huge quantities of chemical additives (traditionally lime and cement), as binders, in many soil stabilization and ground improvement applications. Chemical additives lastingly change the treated soil environment and can cause pollution of groundwater [1]. Biological methods represent promising sustainable and green alternatives, and are broadly classified as (i) methods producing mineral precipitation in the soil pore voids (e.g., bio-grouting); (ii) methods transforming clay minerals from one form to another (i.e., mineral transformation); and (iii) biopolymer-based soil treatment (BBST) [1,2]. To date, bio-grouting technologies in ground improvement applications have mainly employed the microbial-induced calcite precipitation (MICP) process. These applications include increasing the strength/stiffness of sandy soils (e.g., [3–6]), surface soil layer stabilization, fugitive dust control [7–10], and soil permeability reduction [11,12]. In the MICP method, urease positive bacteria, e.g., *Sporosarcina pasteurii* or *Bacillus pasteurii*, create urease enzyme to hydrolyze urea ($CO(NH_2)_2$) into ammonium and carbonate in the company of calcium ions, thereby producing alkalinity that results in calcite crystal

formation, with pH being the main factor governing calcite precipitation [13]. In practice, the field application of the described MICP technique has three main drawbacks. Firstly, for applying the method by reagent injections, the reported optimal soil particle-size distribution is in the range of 0.05 to 0.40 mm [14]. In other words, it is unsuitable (impractical) for treating fine-grained soils because of geometric incompatibility between the bacterial cells (typically sized 0.5–3 μm [15]) and the pore-throat sizes within the soil matrix, which inhibits the bacterial cells from passing between connecting pore spaces [16,17]. Secondly, a relatively non-uniform distribution of precipitated calcite can form in the MICP-treated soil [5], especially at large scale, thereby reducing the potential engineering performance benefits. Thirdly, the efficient soil treatment depth is restricted by the limitation of using aerobic bacteria in deep soils in terms of oxygen deficiency [6,18].

A more recently introduced bio-grouting approach that provides a viable alternative to the MICP method is via enzymatic-induced calcite precipitation (EICP), which uses free urease enzyme (obtained from microorganisms of various plants) to catalyze the urea hydrolysis reaction (e.g., [2,19]). For instance, Dilrukshi and Kavasaki [20] and Dilrukshi et al. [21] reported that watermelon seeds (a urease-rich agricultural waste) achieved optimal results with respect to urea hydrolysis rate and showed favorable pH (of ~pH 8) for precipitation of calcium phosphate compounds. As a new approach, EICP is insufficiently investigated, but it benefits from not having some of the above-mentioned challenges associated with MICP, notably in terms of applying and controlling microbial growth and activity conditions in the soil [18]. For instance, a comparison of EICP- and MICP-treated sand by Nafisi et al. [17] demonstrated that although the average calcite content for MICP treatment was higher than for EICP treatment, a more evenly distributed calcite precipitate was observed for the EICP-treated specimens. Different aspects of the EICP process and its potential for various ground engineering applications have been discussed in several investigations. For elevated calcite precipitation, raised precipitation efficiency and high enzyme-efficiency criteria, Almajed et al. [22] deduced the favored solution composition for EICP soil treatment as 1.0 M urea, 0.67 M calcium chloride ($CaCl_2$), and 3 g/L urease enzyme (with enzyme activity of 3500 U/g) based on results from 37 precipitation tests performed in 50 mL tubes. Yasuhara et al. [23] illustrated that the permeability of EICP-treated sand was more than one order of magnitude smaller than that of untreated (UT) sand specimens, with unconfined compressive strength (UCS) increased up to 1.6 MPa. Moving up the scale, recently Martin et al. [24] reported a large-scale experiment to form a 0.3 m dia. × 0.9 m long EICP-treated sand column within a sand box of 0.6 × 0.6 × 1.2 (L) m dimensions. They injected a cocktail of urea (1.5 M), $CaCl_2$ (1.0 M), 9900 U/L urease enzyme, and 4 g/L nonfat milk powder using 3 injection cycles via a 1.2 m long tube-à-manchette (TAM). For <3% calcite precipitated inside a 0.3 m dia. cylindrical treatment region, they reported a mobilized UCS of >500 kPa measured after 3 days. Overall, their results demonstrated that EICP has promise as a ground improvement method, since it can be devised and implemented in the field for strengthening soil using similar injection methods as conventional permeation grouting techniques. Estimated EICP treatment costs were in the range of USD 60 per cubic meter of sand [24]. However, it should be noted that an unwanted side effect of utilizing both MICP and EICP method is the resulting toxic by-product of ammonium chloride from ureolysis [2].

Relatively minor attention has been given to the application of the EICP technique for stabilization of the surface soil layer to increase water-erosion resistance. Soil erosion produced by hydraulic flow is the main cause of scouring action and failures for underwater geo-structures founded on/in susceptible soil deposits [25]. For instance, this could include the erosion of sandy soil deposits supporting the structural foundations of bridge piers. To meet bridge-deck serviceability requirements, the bearing sandy soil deposit will be in a densified state, either naturally occurring or produced by various ground improvement methods prior to the pier construction. Stabilization of the uppermost sandy soil layer in the pier vicinity is also necessary to increase its hydraulic erosion resistance for mitigating scouring action. The stabilization method could be applied before opening the channel

to water flow. With applications of this nature in mind, and towards developing a more sustainable soil improvement method compared to a traditional pozzolanic binder/grout, this paper presents innovative research investigating the efficacy of the EICP technique to stabilize dense sandy soil for increasing its hydraulic erosion resistance, examined for a wide range of flow velocity. A laboratory investigation is presented on the improvements in hydraulic erosion resistance achieved for compacted (densified) sand specimens mediated using a variety of 10 different EICP treatment protocols, based on single- and two-cycle injections of the urease enzyme and urea–CaCl$_2$ cementation solutions examining a range of cementation solution concentrations. The sand tested was a quartz sand, being the most abundant sand mineralogy worldwide. Surface erosion rates of the UT and EICP-treated sand specimens are determined for various hydraulic shear stress applied to the specimen top surface using the erosion function apparatus (EFA). Compared to, for instance, using various strength testing methods, this experimental approach was deemed more suitable for assessing improvements in surface erosion resistance under hydraulic shear action. Elemental composition and the morphology, spatial distribution, and amount of precipitated calcite in the treated sand specimens are also investigated. The specific aims of this investigation are to:

- Examine the efficacy of the EICP technique for various injection permutations of the reagent solutions in improving the hydraulic erosion resistance of dense medium-gradation sand when tested for high flow velocity conditions.
- Establish the character of the developed microstructures and amount of calcite precipitated for the various EICP treatments employing a range of cementation solution concentrations (0.5 to 1.0 M).
- Explain relative erosion resistance improvements achieved for one/two cycle injections with different injection permutations in terms of precipitated calcite in the crustal sand layer.

2. Experimental Materials and Methods

2.1. Test Sand

Clean, quartz, medium-gradation sand was sourced from the Chirook sand mine located near Chirook village, Deyhuk Rural District, Tabas, Iran. This site was selected for expediency, being used before as a sand source for laboratory investigations by the authors of other biological soil-improvement methods. These included (i) MICP treatment by various reagent-injection strategies [6] and mixing 1–4 wt% nano-silica additive [26] for dense medium sand, (ii) inoculation of fine, medium, and medium–coarse gradation sands with cyanobacteria [27,28] to improve their hydraulic erosion resistances, (iii) the bio-cementation of the loose medium-gradation surface sand layer employing the MICP technique, by spray application, for mitigating wind-induced erosion [10].

The test sand used in the present investigation comprised sub-angular grains ranging 0.125 to 0.50 mm in particle size (see Figure 1). The grading curve was determined by the dry sieving method. With D_{10}, D_{30}, and D_{60} (i.e., particle sizes corresponding to 10, 30, and 60 wt% passing) of 0.17, 0.22 and 0.30 mm, respectively, the test sand had coefficients of uniformity C_U (=D_{60}/D_{10}) and curvature C_C (= $D_{30}^2/D_{60} D_{10}$) values of 1.76 and 0.95, respectively. According to the experimental grading curve, the mean particle size (D_{50}) was 0.28 mm. Using the pycnometer method, the specific gravity of the solid particles was measured as 2.67, and the minimum and maximum dry densities were measured as $\rho_{d\ min}$ = 1.40 Mg/m^3 and $\rho_{d\ max}$ = 1.66 Mg/m^3, as determined using a funnel pouring device and vibratory table, respectively.
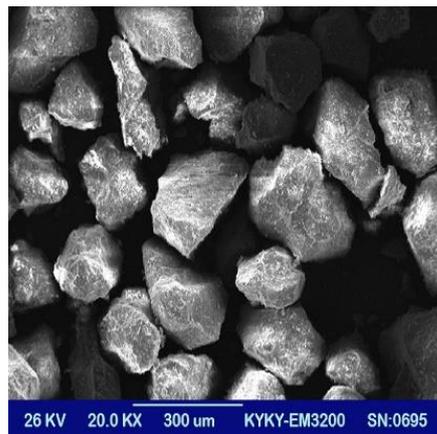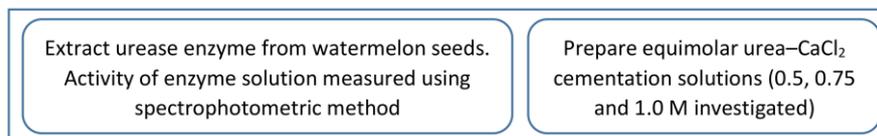
Figure 1. Scanning electron microscope (SEM) image of untreated (UT) test sand.

2.2. Preparation of EFA Test Specimens and Applying EICP Treatment

This section describes the sequence of actions in preparing the EICP-treated dense sand specimens for EFA testing (overview of process presented in Figure 2). As described in the Introduction, the authors had identified the application of the EICP technique for mitigating the scouring of dense load-bearing sandy soil deposits as a gap in the research literature. In addition, the precipitated calcite in EICP-treated specimens was analyzed in term of (i) elemental composition and crystal structure using X-ray diffraction (XRD) examination, (ii) morphology and spatial distribution among the sand matrix by SEM examination, and (iii) quantity of precipitated calcite determined using the gravimetric acid-washing method.

Urease Enzyme and Cementation Solutions

Extract urease enzyme from watermelon seeds. Activity of enzyme solution measured using spectrophotometric method
Prepare equimolar urea–CaCl$_2$ cementation solutions (0.5, 0.75 and 1.0 M investigated)

Preparation of EFA test-specimes

Fill specimen molds with clean dry sand compacted in three equal-height layers (density index of 0.75). Top specimen surface protrudes 1-mm above mold rim

Flush air from pore-void spaces by downward seepage of distilled water introduced onto specimen top surface, with drainage via bottom port

Urease enzyme solution introduced onto specimen top surface, excess draining away via bottom port to peristaltic pump

After 15 min, cementation solution introduced in same manner, with excess solution ponded on specimen top surface

Six days after first injection cycle, some test-specimens receive second cycle of enzyme and/or cementation solution(s) (refer to Table 1)

Once treated, specimen molds (with excess cementation solution ponded on top surface) placed in sealed plastic bags and cured in incubator at 50°C for 14-day period
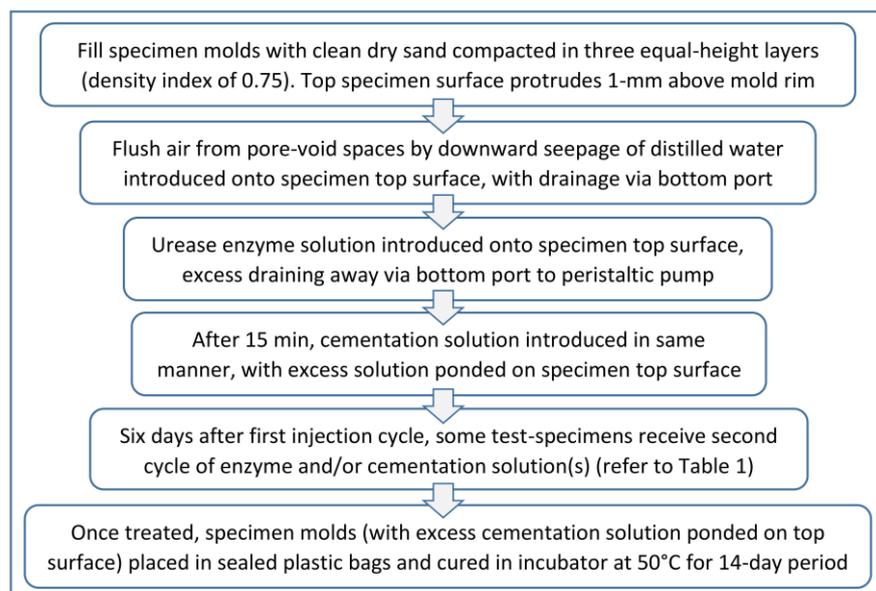
Figure 2. Flow chart of specimen making process.

2.2.1. Preparing Cementation and Urease-Enzyme Solutions

As cementation solution, equimolar urea–CaCl$_2$ solutions were prepared at three concentrations of 0.5, 0.75, and 1.0 M. For this study, the urease enzyme was extracted from watermelon seeds via a process of crude extraction, achieved by blending, filtration, and centrifugation, and two-stage purification, as described in Javadi et al. [19]. The test for urease activity was performed using the spectrophotometric method for absorbance at a wavelength of 560 nm [21,29]. Enzyme activity is the quantity of enzyme that is able to release one micromole of ammonia per minute. In order to measure the enzyme activity, the calibration curve in Figure 3 was first obtained for different concentrations (0.08, 0.06, 0.04, 0.02, and 0.10 M/L) of 0.5 M ammonium carbonate solution in 0.01 M phosphate buffer dissolved with a concentration of 20 µg/mL of phenol red. The prepared solutions were poured into the microplate houses in the amount of 100 µL and their absorbance measured at a wavelength of 560 nm employing a Citation device, as plotted in Figure 3. Next, a solution of 20 mM phosphate buffer, phenol red, and 0.5 M urea was prepared and then added to the extracted enzyme solution for measurement of its activity. The samples were incubated at temperatures of 30 and 50 °C and their absorption read for different incubation periods (Figure 4). Using the data of the calibration curve and enzyme activity diagram of the extracted urease enzyme, the amount of enzyme activity was determined as 2400 and 2800 U/L for 30 and 50 °C, respectively.
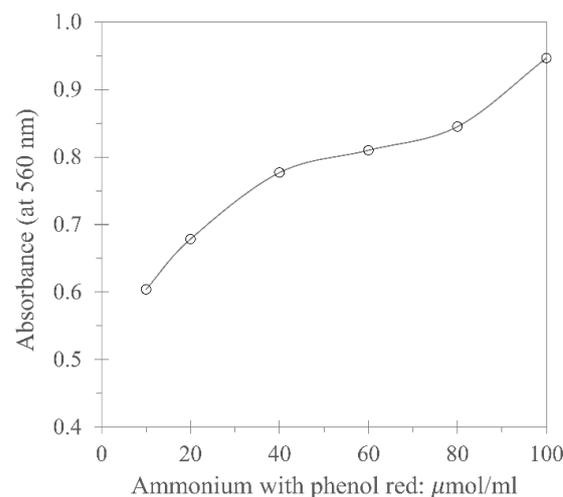

Figure 3. Calibration plot for change in absorbance at a wavelength of 560 nm measured by spectrophotometer.
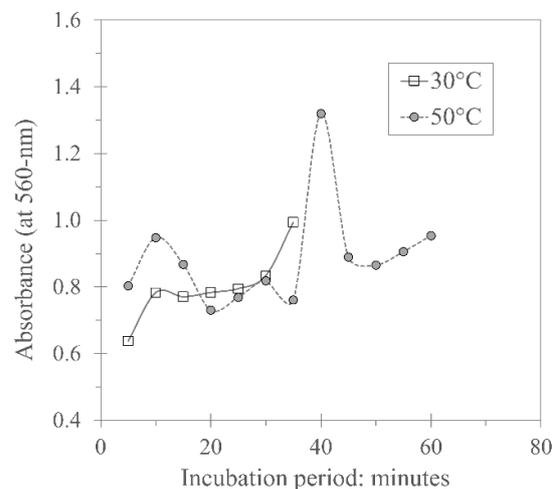

Figure 4. Change in absorbance at 560 nm wavelength with incubation at 30 and 50 °C.

2.2.2. Preparing Dense Sand Test Specimens

Clear plastic containers (specimen molds) of 66 mm internal diameter at the top rim and with 228.5 mL internal volume capacity were used to hold the sand specimens for performing the EFA testing. An extension collar of plastic film was wrapped around, and secured using an elastic band to form a watertight seal on, the threaded outer top rim of the specimen container (see Figure 5), with two purposes. Firstly, to allow the preparation of sand specimens that protruded slightly (i.e., a distance of 1-mm) above the containers' rim and, secondly, for ponding of water, cementation solution, or urease enzyme solution on the specimen's top surface to cause downward flow to occur through the pore void spaces. A side drainage port was fitted at the bottom of each container (see Figure 5a). The washed and oven-dried sand material was placed in three equal-height layers to fill the specimen containers to a height of 1-mm above the rim level, each layer tamped to achieve a density index of $I_D = 0.75$ (dry density of 1.59 Mg/m^3) for the prepared test specimens (i.e., dense state). From the computed specimen void ratio of 0.68 (porosity of 40.4%), the volume of the specimen pore-void spaces, V_v (i.e., the specimen water-holding capacity) was determined as 92.6 mL.
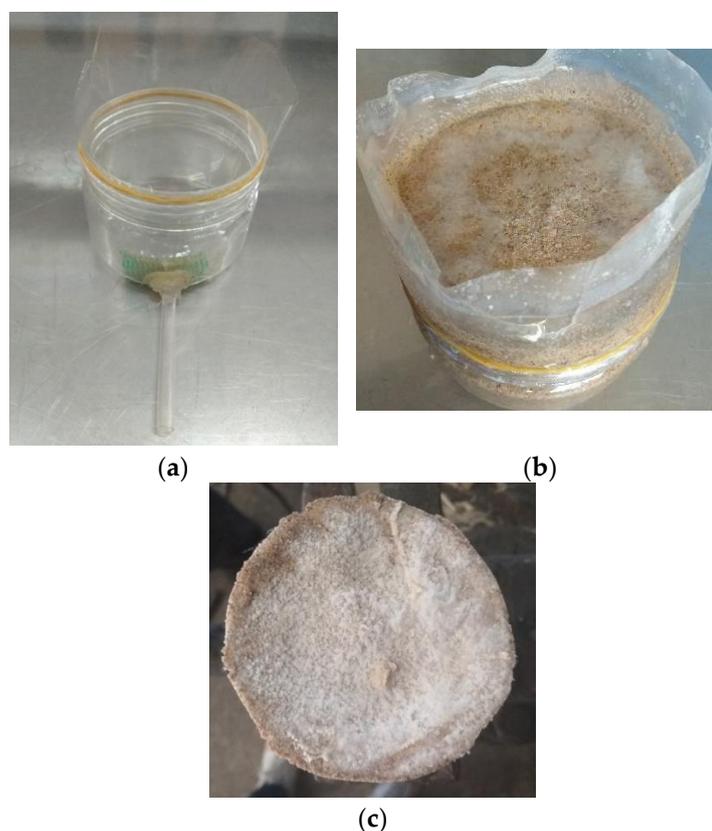

(a) (b)

(c)

Figure 5. (**a**) Specimen container fitted with side drainage port and plastic-film extension collar fitted around top rim. (**b**,**c**) side and top views of white calcite deposits visible on surface of 14-day cured EICP-treated sand specimen.

For the purpose of de-airing the test specimens, distilled water was carefully introduced onto their top surface. With the bottom drainage port open, the water seeped down through each test-specimen to flush the air from the pore-void spaces.

2.2.3. EICP Treatment of Sand Test Specimens

The urease enzyme and cementation solutions were introduced onto the exposed top surface of the test specimens (i.e., no pressure head was applied to drive the flow), with excess liquid allowed to drain away via the bottom port to a peristaltic pump. First, the

enzyme solution of 50-mL volume (i.e., $\sim V_v/2$) was introduced. After a 15-min period that allowed this solution to filter and distribute over the specimen length, cementation solution of 100-mL volume (i.e., $\sim 1.1 \times V_v$) was introduced in the same manner, with excess solution (i.e., $0.1 \times V_v$) ponded on (above) the specimen top surface. Six days after this first injection cycle, some test specimens received a second injection cycle of enzyme and/or cementation solution(s). Taking protocol J as an example (and referring to Table 1), injections of 50 mL enzyme solution followed 15-min later by 100 mL 1.0-M cementation solution were introduced on Day 1, with the same injection cycle repeated on Day 7. Once treated, the containers (with the excess volume of cementation solution ($\sim 0.1 \times V_v$) ponded on the specimen top surface) were placed in sealed plastic bags to prevent air exposure and drying, and the specimens were then allowed to cure in an incubator at 50 °C over a 14-day period before performing the EFA testing (i.e., on Day 14). All EICP-treated specimens were injected with urease enzyme (4 g/L), phosphate buffer (50 mL) and equimolar urea–CaCl$_2$ cementation solution (pH $\approx$ 8).

Table 1. Reagent injections for 10 different EICP treatment protocols investigated in present study.

Treatment Protocol	A	B	C	D	E
Day 1	Enzyme and 0.5-M cementation solutions	Enzyme and 0.75-M cementation solutions	Enzyme and 1.0-M cementation solutions	Enzyme and 0.5-M cementation solutions	Enzyme and 0.75-M cementation solutions
Day 7	–	–	–	Enzyme solution	Enzyme solution
Treatment Protocol	**F**	**G**	**H**	**I**	**J**
Day 1	Enzyme and 1.0-M cementation solutions	Enzyme and 0.5-M cementation solutions	Enzyme and 0.75-M cementation solutions	Enzyme and 1.0-M cementation solutions	Enzyme and 1.0-M cementation solutions
Day 7	Enzyme solution	0.5-M cementation solution	0.75-M cementation solution	1.0-M cementation solution	Enzyme and 1.0-M cementation solutions

2.2.4. EICP Treatment Protocols Investigated

Altogether, 10 different EICP treatment protocols (labelled A to J in Table 1) were examined, with the aims of establishing an optimum injection strategy to achieve significant calcite precipitation and distribution, and hence improved erosion resistance, for the EICP treated sand. Referring to Table 1, protocols A–C involved a single enzyme–cementation solutions injection cycle, whereas protocols D–J included second urease enzyme and/or cementation solution injections. Comparing experimental results for protocols A–C would allow examination of the effect of cementation solution concentration (0.5, 0.75, and 1.0 M) for the EICP treated sand. The other protocols (D–J) were grouped according to the solution type(s) used for the second injection cycle applied after the 6-d standing period. That is, for the second injection cycle, protocols D–F used only enzyme solution, protocols G–I used only cementation solution (at the three different concentrations), while both enzyme and cementation solutions were injected for protocol J. Additionally, some UT specimens were EFA tested, and acted as controls to allow comparisons of relative erosion resistance improvements achieved between the 10 EICP protocols investigated.

2.3. Calcite Formation, Content and Distribution for EICP Treated Specimens

XRD examination was performed to determine the elemental composition and crystal structure of the precipitates formed in specimens treated using protocols C and J (i.e., single- and two-cycle enzyme–1.0-M cementation solutions injections, respectively). SEM examination using a TESCAN-vega3 apparatus run in high-vacuum mode (20 kV) was used to investigate the morphology and spatial distribution of the calcite crystals formed in the pore-void spaces.

For EICP treated test specimens, the gravimetric acid-washing method was utilized to investigate the quantity of calcite precipitated in forming (stabilizing) the crustal sand layer. Since most of the treated specimens also had calcite deposits formed on their top surface

(see Figure 5b,c), thin disc samples of the stabilized sand were cut from just below the specimen top end (see Figure 6) and the amounts of calcite precipitation therein measured using calcium-carbonate titration tests, as follows. One gram of dry EICP-treated sand (i.e., W_{soil}) was carefully poured into a 250 mL flask. A total of 25 mL (i.e., V_{HCl}) of 0.5 normal (i.e., N_{HCl}) hydrochloric acid was added and then heated to the boiling point. The solution was filtered with 42-Grade filter paper and its soil contents were washed with 50 mL of boiled distilled water. A few drops of phenolphthalein were added to the filtered solution and titrated (i.e., V_{NaOH}) with 0.25 normal (i.e., V_{NaOH}) sodium hydroxide until it achieved a purple color, and the Burt number was noted. The percentage of soil calcium-carbonate was calculated as follows:

$$\% \text{ CaCO}_3 = \frac{(V_{HCl} \times N_{HCl}) - (V_{NaOH} \times N_{NaOH})}{W_{soil}} \times 5 \tag{1}$$

Figure 6. Disc sample (**left**), cut from top of EICP-treated sand specimen (**right**), used in investigating amounts of calcite precipitation.

2.4. EFA Testing

The Shiraz University's EFA device (see Figure 7) was used to measure the surface erosion rate of EICP-treated and UT sand specimens. This EFA device has a 2.0 m long conduit having 12 cm wide × 6 cm high cross-sectional dimensions internally. A distance of 1.3 m along the conduit (from the inlet side), a specimen container can be secured in a 6.5 cm dia. opening centered on its base dimension (Figure 7a). The exposed specimen top surface was positioned to protrude a distance of 1-mm above the inside surface of the conduit bottom wall. The containers' threaded top rim (see Figure 5) allowed its screw attachment and achieving a watertight seal to the conduit base, and also for fine positioning of the amount of specimen protrusion.

The inlet valve to the conduit (Figure 7c) controls the direction of the water flow, i.e., to occur along or bypass the conduit, and allows adjustment of the flow rate. Past the conduit outflow, a triangular weir and point gauge arrangement located at the end of a channel (see Figure 7e) permits measurement of the flow rate. Once the flow discharge was adjusted to achieve the desired mean flow velocity (V), the inlet value was opened to allow the flow to occur along the conduit length. The time interval (Δt) from opening this valve to complete removal of the protruding 1-mm-tall sand layer was measured using a chronometer. A window in the conduit sidewall (Figure 7d) allowed inspection of the specimen erosion rate during the EFA tests. The inlet valve was then closed to redirect the flow away from the conduit, with remaining water within the conduit allowed to drain away to the channel end. Finally, the specimen container was carefully removed from the bottom of the conduit. For each EICP treatment protocol investigated, the experiment was repeated in triplicate on identically prepared test specimens for three different mean flow

velocity values, measuring the times required to erode and remove the protruding 1-mm tall sand layer when subjected to three different tangential shear stress.
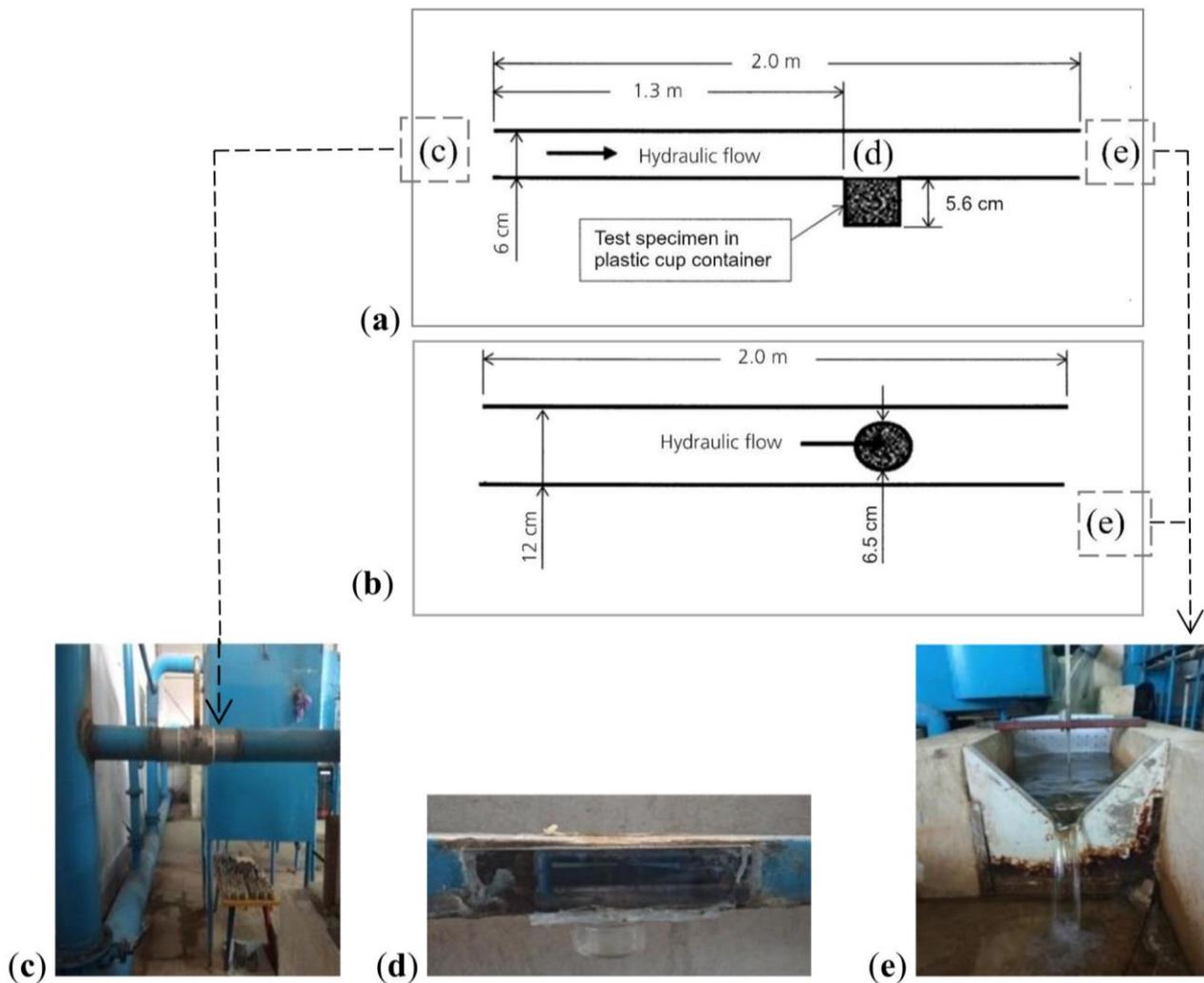

Figure 7. EFA testing device: (**a**) long cross-section and (**b**) plan view diagrams of 2-m long conduit; (**c**) inlet valve located near conduit inlet; (**d**) side window for viewing bare top surface of test specimen contained in plastic holder secured to conduit bottom wall; (**e**) point gauge and triangular weir flow-measurement method (Reprinted with permission from Rabiei et al. [27]. 2022, ICE Publishing).

3. Experimental Results and Analyses

3.1. XRD and SEM

Being a clean quartz sand, no calcite was detected in the XRD results for the UT specimen. Whereas the XRD trace for the protocol-J-treated sand specimen indicated calcite mineral precipitation had occurred as a result of the EICP reactions. Figure 8 presents SEM images at different magnification showing grains of the UT sand (Figure 8a–c) and treated sand using the C (Figure 8d–f) and J (Figure 8g–i) protocols of single- and two-cycle enzyme–1.0-M-cementation solutions injections, respectively. For treated specimens, distinct calcite crystal precipitation covering individual sand grains and causing almost complete filling of the pore-void spaces is evident. While Figure 8g–i for protocol J of two-cycle enzyme–1.0-M cementation solutions injections indicates large calcite crystals, formed integrated in the pore-void spaces, produces greater void filling compared to protocol C (i.e., single-cycle of enzyme–1.0-M-cementation solutions injections), which is shown in Figure 8d–f. In other words, the net effect for the EICP-treated sand specimens is a cementing (binding together) of the individual sand grains to form a crustal layer with significantly reduced void ratio.

The latter would also result in significant reductions in the permeability coefficient (not measured in the present study).
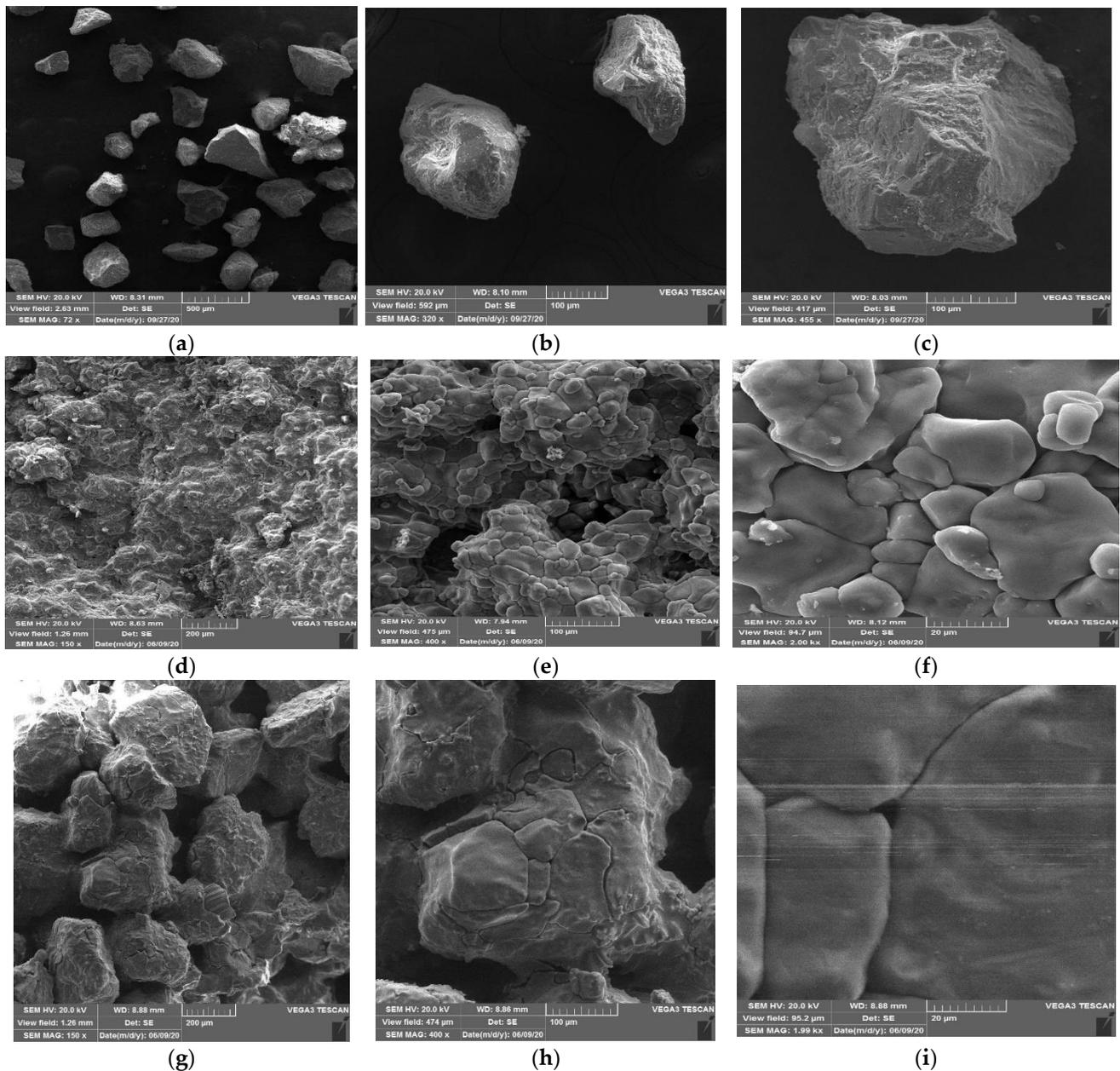

Figure 8. SEM images at different magnification for (**a**–**c**) untreated sand and EICP-treated sand using protocol C (**d**–**f**) and protocol J (**g**–**i**). Refer to Table 1 for summaries of these treatment protocols.

3.2. Calcite Content Precipitated for Different EICP Treatment Protocols

Figure 9 shows the average calcite content of the formed crustal sand layer (i.e., top end section of the test specimen where solutions were introduced) measured for all 10 EICP treatment protocols investigated. From this figure, the largest calcite content of 18.7 wt% was achieved for protocol J (two cycles of enzyme–1.0-M-cementation solutions injections), as compared to only 5.0 wt% for protocol F (two-cycle injection protocol with enzyme–1.0-M-cementation solutions used in the first cycle but only enzyme solution injected in the second cycle). This range in the amounts of calcite precipitate for the uppermost sand layer is comparable with that achieved for MICP treated dense sand specimens of the same medium sand investigated in Amin et al. [6]. For instance, 15.5 wt% calcite was precipitated in the uppermost sand layer for two cycles of bacterial cell–0.75-M-cementation solutions

injections, compared to 6.7 wt% calcite precipitated for a single cycle of bacterial cell–0.5-M cementation solutions injections [6].
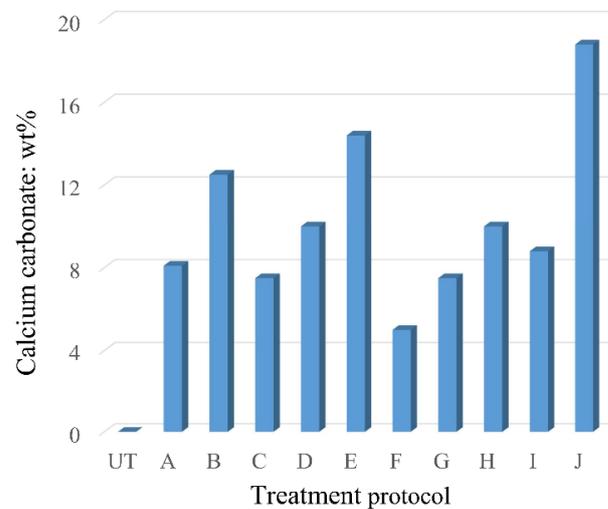

Figure 9. Relative performance of EICP treatment protocols in terms of calcite precipitation. Refer to Table 1 for summaries of the treatment protocols.

3.3. EFA Results and Analysis

The experimental results for all 10 EICP treatment protocols investigated are plotted in Figure 10 as erosion rate (E) versus hydraulic shear stress (τ) acting at the water–sand interface. The E and τ magnitudes were computed as follows

$$E = \frac{V_e}{A_s \, \Delta t} \tag{2}$$

$$\tau = \frac{1}{8}\rho_w f V^2 \tag{3}$$

where V_e = eroded sand volume (i.e., protruding 1-mm-tall sand layer), A_s = specimen cross-sectional area (constant), Δt = time interval from opening conduit inlet valve to complete removal of protruding sand layer, V = mean flow velocity, ρ_w = density of water, f = friction factor obtained from the Moody chart [30].
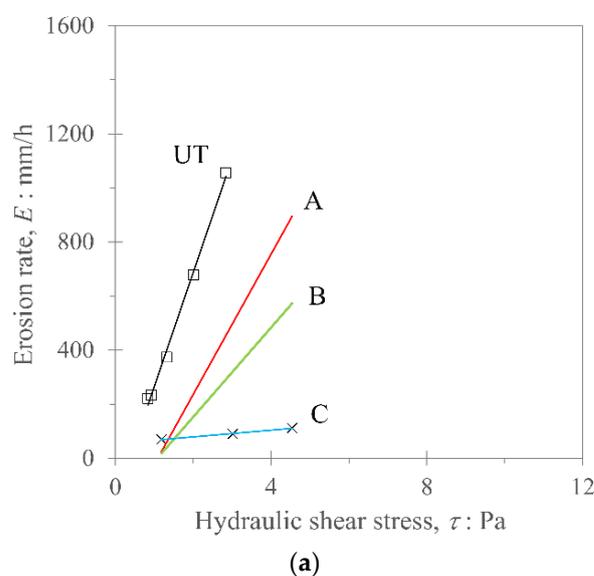

(a)

Figure 10. *Cont.*
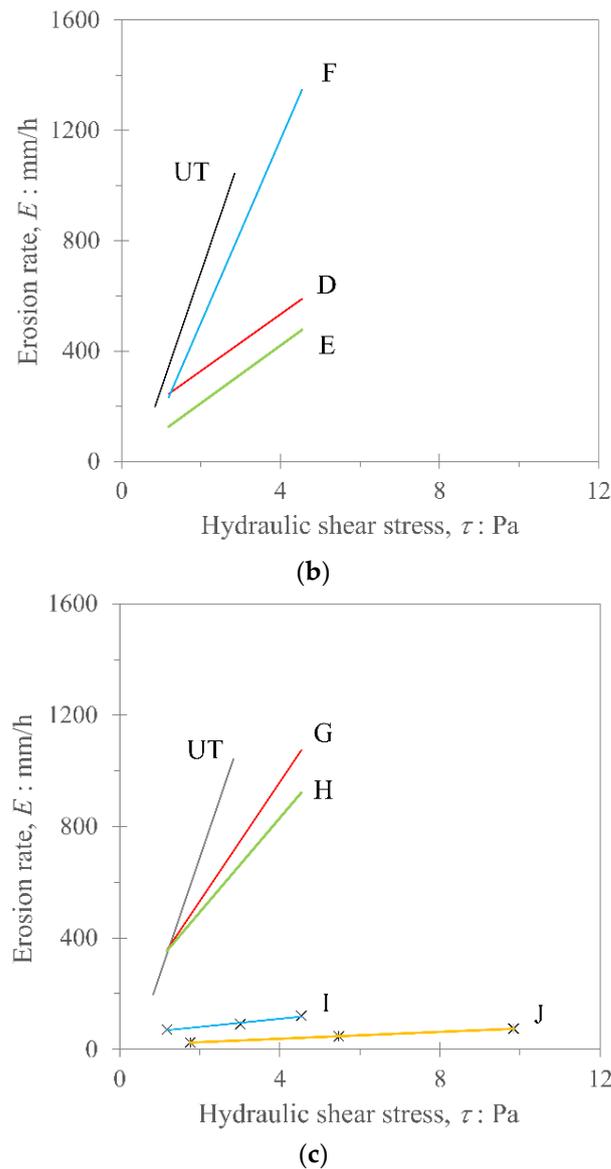
(b)

(c)

Figure 10. Erosion charts for various EICP treatments: (**a**) protocols A–C; (**b**) protocols D–F; (**c**) protocols G–J (refer to Table 1 for descriptions of the different protocols). Note: UT, untreated sand.

For applying the Moody chart, which correlates f to Reynold's number (R_e) and relative roughness (ε'), these experimental parameters were estimated as follows

$$R_e = \frac{VD}{\nu} \tag{4}$$

$$\varepsilon' = \frac{0.5 \times D_{50}}{D} \tag{5}$$

where ν = kinematic viscosity of water (at 20 °C), D = hydraulic diameter of the rectangular conduit, D_{50} = mean particle size (of sand tested).

Erosion resistance was measured in terms of the erosion coefficient (K_τ), determined as the gradient of the best-fit linear regression line in the experimental E–τ chart, and the erodibility threshold (i.e., critical hydraulic shear stress τ_c), determined as the intersection point of the extrapolated regression line with the horizontal (τ) axis. That is, soil erosion occurs when the tangential shear stress of the flow surpasses the critical shear stress τ_c. Table 2 lists the computed K_τ and τ_c values for the 10 EICP treatment protocols, along

with their K_τ reductions calculated relative to the UT sand. With $\tau_c < 1$ Pa, the UT sand is categorized as having very high erodibility [31].

Table 2. EFA results for various EICP treatment protocols examined.

Treatment Protocol	Critical Shear Stress, τ_c (Pa)	Erosion Coefficient, K_τ (mm/h/Pa)	% Reduction in K_τ (Relative to Control)
A	1.2	260	38.4
B	1.7	178	57.8
C	2.2	12.5	97.0
D	1.2	123	70.8
E	2.0	105	75.2
F	1.0	332	21.2
G	1.5	214	49.3
H	1.1	169	59.9
I	1.9	14.5	96.6
J	1.0	6.2	98.6
UT (control)	0.4	422	–

Referring to Table 2 and Figure 10, compared to UT sand, all 10 EICP treatment protocols produced an increase in τ_c (by approx. three- to six-fold) and also a reduction in K_τ, thereby significantly enhancing the surface layer's erosion resistance. This was especially the case with employing higher molar (i.e., 1.0 M) cementation solution for single- and two-cycle enzyme–cementation solutions injections (i.e., protocols C and J), which achieved >97% K_τ reductions.

Comparing results for protocols A, B, and C (i.e., single injection cycle of enzyme solution and 0.5, 0.75, and 1.0 M cementation solution, respectively) indicates increasing K_τ reductions from 38.4% to 57.8% to 97.0%, respectively, were achieved for increasing cementation solution concentration.

Protocols D–J included a second injection cycle (applied 6 days after the first one) and, for the purposes of analyzing the EFA test results, are grouped according to solution type(s) injected in the second cycle. First, the results for the two-cycle injection protocols D, E, and F (with increasing cementation solution concentration used in the first cycle of 0.5, 0.75, and 1.0 M, respectively, but only enzyme solution injected in the second cycle) are compared. Protocols D and E achieved K_τ reductions of 70.8 and 75.2%, respectively, whereas protocol F (i.e., employing 1.0-M cementation solution) merely produced a 21.2% K_τ reduction. Poorer performance for protocol F may be related to the negative feedback mechanism in the urea hydrolysis reaction on enzyme activity (discussed in Section 4).

Next, comparing the EFA test results for the two-cycle injection protocols G, H, and I (with the second injection cycle introducing only cementation solution (of 0.5, 0.75, and 1.0 M concentration, respectively)) indicates increasing K_τ reductions of 49.3, 59.9, and 96.6%, respectively, were again achieved for higher cementation solution concentration. Comparing the EFA test results for protocols G and A indicates that the second injection of 0.5-M cementation solution applied for protocol G produced a larger K_τ reduction (of 49.3%, compared to 38.4% for protocol A). Whereas comparison of protocols H and B indicates that the second injection of 0.75-M cementation solution did not produce substantiate further reductions in the K_τ magnitude achieved for one-cycle injection. This was also the case for comparing the EFA test results for protocols I with C, which both employed 1.0-M cementation solution. Finally, protocol J (employing two-cycle enzyme–1.0-M-cementation solutions injections) achieved the largest K_τ reduction of 98.6%.

4. Discussion and Recommendations for Future Research

As evidenced from the SEM observations (Figure 8), the EICP-treatment produced a calcite precipitate that cemented (bound together) individual sand grains and caused significant reductions in the void ratio, and hence in the permeability coefficient. Compared to UT sand, protocol J (two cycles of enzyme–1.0-M-cementation solutions injections)

achieved the largest K_τ reduction of 98.6%, closely followed by 97.0% for protocol C (single-cycle of enzyme–1.0-M-cementation solutions injections) and 96.6% for protocol I (two-injection cycles but introducing only 1.0-M cementation solution for the second cycle) (refer to Table 2). In other words, in terms of overall efficacy, the bench-scale experimental results indicate that protocols C, I, and J achieved comparable performances, and of these three, the single cycle of enzyme–1.0-M-cementation solutions injections is the more pragmatic option. For both single- and two-cycle cementation solution injections, significantly larger K_τ reductions were generally achieved for increasing cementation solution concentration (0.5 to 1.0 M range investigated). Exceptions were two-cycle injections where the second cycle involved injecting only cementation solution at 0.75 or 1.0 M concentration (i.e., no enzyme solution introduced for second cycle). Here, the magnitude of K_τ reductions were similar to those achieved for single-cycle injection at the same cementation solution concentration. A plausible explanation is that this may be related to the ratio of the amounts of urease enzyme and cementation solution present, so that with increasing cementation solution concentration more hydrolysis of urea requires increasing the amount of enzyme. Among the 10 investigated protocols, treatment protocol F (two-cycle injection with 1.0-M cementation solution employed in the first cycle, but only enzyme solution introduced in the second cycle) produced the least improvement in the erosion resistance (only 21.2% K_τ reduction compared to control). This possibly happened because of the negative feedback mechanism in the urea hydrolysis reaction on enzyme activity. In other words, for the 1.0-M cementation solution with two-cycle enzyme solution injections, a lack of ambient calcium for reacting with high carbonate ion production in urea hydrolysis arose.

Protocol-J-treated sand had the highest amount of precipitated calcite at 18.7 wt% and, as described above, it was also the best performing in the EFA tests, producing a 98.6% K_τ reduction. Whereas protocol-F-treated sand had the lowest precipitated calcite of 5.0 wt%, being the worst performing of the EFA test specimens, achieving only a 21.2% K_τ reduction. The SEM images presented in Figure 8d–i for protocols C and J visually corroborate higher amounts of precipitated calcite, producing larger calcite crystal formation and greater filling of the pore-void spaces for protocol J (comprising two cycles of enzyme–1.0-M-cementation solutions injections compared to the single injection cycle employed for protocol C). However, assessing likely erosion resistance performance based solely on precipitated calcite content is not always sufficient. For instance, protocols J, C, and I achieved comparatively large K_τ reductions, yet the sand specimens produced for injection protocols C and I had substantially lower precipitated calcite contents of 7.5 and 8.8 wt%, respectively. In other words, the spatial distribution of the precipitated calcite in treated sand is another very important consideration. Examination of the EICP-treated sand for protocols J and C indicated precipitated calcite completely covered the sand grains, binding them together and almost completely filled the pore-void spaces, especially for the two-cycle injection protocol J.

Additional laboratory testing and especially pilot field studies are suggested to corroborate the experimental results of this study, and to examine their relation and broadening to natural environments in larger scales, considering feasible approaches of applying the EICP treatment technology in engineering practice. Pertinent questions include the overall effectiveness of EICP treatment in the real environment and also its longevity. For instance, the study tested distilled water, but natural water is not as pure, such that when the EICP treatment is used, various effects, particularly on chemical reactions, exist. Aside from EFA testing (preferred laboratory approach), the bench-scale experimentation could also involve, for example, strength testing of the stabilized sand layer employing pocket penetrometer or Torvane devices (e.g., [10,27]).

5. Summary and Conclusions

This paper presented a laboratory investigation of the improvements in hydraulic erosion resistance achieved for dense, medium-gradation quartz sand specimens mediated using 10 different EICP treatment protocols. Fifteen minutes after injection of the enzyme

solution, with urease activity of 2400 U/L measured at 30 °C, the equimolar urea–CaCl$_2$ cementation solution (at 0.5, 0.75, or 1.0 M concentration) was injected. A second injection cycle was also investigated for a 6-day standing period between the first and second injection cycles. Treated test specimens were cured at 50 °C for a 14-day period and then subjected to various hydraulic shear stress to cause erosion of the crustal sand layer investigated using an EFA device.

SEM observations revealed the precipitated calcite from EICP treatment cemented (bound together) the individual sand grains and produced significant reductions in the void ratio, and hence in the permeability coefficient. Compared to UT sand, all 10 EICP treatment protocols produced substantially increased τ_c (by approx. three- to six-fold) and also reduced K_τ, thereby significantly enhancing the surface sand layer's erosion resistance, as assessed using EFA testing. Significantly larger K_τ reductions were generally achieved for increasing cementation solution concentration. The largest K_τ reductions (of ~97–99%) were achieved for single-cycle enzyme–1.0-M-cementation solutions injections, and two-cycle injection utilizing 1.0-M cementation solution with/without enzyme solution introduced for the second cycle. Of these, single-cycle enzyme–1.0-M-cementation solutions injections was identified as the more pragmatic option (i.e., only one reagent injection cycle needed). At high cementation solution concentration (1.0 M), double injection of enzyme solution caused a negative feedback mechanism, reducing enzyme activity, and thereby producing the least K_τ reduction (of only 21.2%) among all EICP treated specimens.

The highest and lowest amounts (18.8 and 5.0 wt%) of precipitated calcite corresponded to the best and worst performing EICP-treated specimens in the EFA tests. However, assessing likely erosion resistance performance based solely on precipitated calcite content was not always sufficient, with the spatial distribution of precipitated calcite in treated sand being another important factor. Since the strength of EICP-treated sand depends on the urease activity, further laboratory studies are recommended to study the efficacy of the various treatment protocols investigating higher activity of urease enzyme. This controlled experimental laboratory study is an initial step towards developing a more sustainable soil improvement method compared to using a traditional pozzolanic binder/grout. Pilot field studies are recommended to examine broadening of the laboratory results to natural environments, including investigations of feasible approaches to apply the EICP treatment technology in engineering practice for sizable land areas.

Author Contributions: Conceptualization, S.M.A.Z.; methodology, S.M.A.Z.; validation, B.C.O. and S.M.A.Z.; formal analysis, B.C.O., H.G., S.M.A.Z. and S.N.; investigation, S.N.; writing—original draft preparation, H.G.; writing—review and editing, B.C.O. and S.M.A.Z.; visualization, B.C.O., S.M.A.Z. and S.N.; supervision, S.M.A.Z.; funding acquisition, S.M.A.Z. All authors have read and agreed to the published version of the manuscript.

Institutional Review Board Statement: Not applicable.

Informed Consent Statement: Not applicable.

Data Availability Statement: The original experimental data presented in the paper is available from the corresponding authors subject to reasonable request.

Conflicts of Interest: The authors declare no conflict of interest.

Abbreviations

EICP	enzymatic-induced calcite precipitation
EFA	erosion function apparatus
MICP	microbial-induced calcite precipitation
SEM	scanning-electron microscope
UT	untreated (specimen)
XRD	X-ray diffraction

Notations

A_s	cross-sectional area of test-specimen
C_C	coefficient of curvature
C_U	coefficient of uniformity
D	hydraulic diameter (of EFA conduit)
D_{10}	effective grain size
D_{30}	particle size for 30 wt% passing
D_{50}	mean particle size
D_{60}	particle size for 60 wt% passing
E	erosion rate
f	friction factor
K_τ	erosion coefficient (retrieved from E–τ chart)
R_e	Reynold's number
V	mean flow velocity
V_e	eroded sand volume
V_v	volume of specimen pore voids
Δt	time interval
$\varepsilon\prime$	relative roughness
$\rho_{d\,min}$	minimum dry density
$\rho_{d\,max}$	maximum dry density
ρ_w	density of water
τ	hydraulic shear stress acting at soil–water interface
τ_c	critical shear stress
ν	kinematic viscosity

References

1. Sujatha, E.R.; O'Kelly, B.C. Biopolymer based soil treatment for geotechnical engineering applications. In *Handbook of Biopolymers*; Thomas, S., AR, A., Jose, C.C., Thomas, B., Eds.; Springer: Singapore, 2023; p. 18. [CrossRef]
2. Assadi Langroudi, A.; O'Kelly, B.C.; Barreto, D.; Cotecchia, F.; Dicks, H.; Ekinci, A.; Garcia, F.E.; Harbottle, M.; Tagarelli, V.; Jefferson, I.; et al. Recent advances in nature inspired solutions for ground engineering (NiSE). *Int. J. Geosynth. Ground Eng.* **2022**, *8*, 3. [CrossRef]
3. Van Paassen, L.A.; Harkes, M.P.; van Zwieten, G.A.; van der Zon, W.; van der Star, W.; van Loosdrecht, M. Scale up of BioGrout: A biological ground reinforcement method. In Proceedings of the 17th International Conference on Soil Mechanics and Geotechnical Engineering, Alexandria, Egypt, 5–9 October 2009; Hamza, M., Shahien, M., El-Mossallamy, Y., Eds.; IOS Press: Amsterdam, The Netherlands, 2009; Volume 3, pp. 2328–2333.
4. Al Qabany, A.; Soga, K.; Santamarina, C. Factors affecting efficiency of microbially induced calcite precipitation. *J. Geotech. Geoenviron. Eng.* **2012**, *138*, 992–1001. [CrossRef]
5. Shahrokhi-Shahraki, R.; Zomorodian, S.M.A.; Niazi, A.; O'Kelly, B.C. Improving sand with microbial-induced carbonate precipitation. *Proc. Inst. Civ. Eng. Ground Improv.* **2015**, *168*, 217–230. [CrossRef]
6. Amin, M.; Zomorodian, S.M.A.; O'Kelly, B.C. Reducing the hydraulic erosion of sand using microbial-induced carbonate precipitation. *Proc. Inst. Civ. Eng. Ground Improv.* **2017**, *170*, 112–122. [CrossRef]
7. Bang, S.S.; Bang, S.; Frutiger, S.; Nehl, L.M.; Comes, B.L. Application of novel biological technique in dust suppression. In Proceedings of the Transportation Research Board 88th Annual Meeting, Washington, DC, USA, 11–15 January 2009; Transportation Research Board: Washington, DC, USA, 2009; p. 13.
8. Meyer, F.D.; Bang, S.; Min, S.; Stetler, L.D.; Bang, S.S. Microbiologically-induced soil stabilization: Application of *Sporosarcina pasteurii* for fugitive dust control. In Proceedings of the Geo-Frontiers Congress 2011, Dallas, TX, USA, 13–16 March 2011; Han, J., Alzamora, D.E., Eds.; ASCE: Reston, VA, USA, 2011. GSP 211. pp. 4002–4011. [CrossRef]
9. Anderson, J.; Bang, S.S.; Bang, S.; Lee, S. Application of microbial calcite to fiber reinforced soils to reduce wind erosion potential. *Int. J. Geo-Eng.* **2012**, *4*, 47–54.
10. Zomorodian, S.M.A.; Ghaffari, H.; O'Kelly, B.C. Stabilisation of crustal sand layer using biocementation technique for wind erosion control. *Aeolian Res.* **2019**, *40*, 34–41. [CrossRef]
11. Dennis, M.L.; Turner, J.P. Hydraulic conductivity of compacted soil treated with biofilm. *J. Geotech. Geoenviron. Eng.* **1998**, *124*, 120–127. [CrossRef]
12. Seki, K.; Miyazaki, T.; Nakano, M. Effects of microorganisms on hydraulic conductivity decrease in infiltration. *Eur. J. Soil Sci.* **1998**, *49*, 231–236. [CrossRef]
13. Stocks-Fischer, S.; Galinat, J.K.; Bang, S.S. Microbiological precipitation of $CaCO_3$. *Soil Biol. Biochem.* **1999**, *31*, 1563–1571. [CrossRef]

14. Rebata-Landa, V. Microbial Activity in Sediments: Effects on Soil Behavior. Ph.D. Thesis, Georgia Institute of Technology, Atlanta, GA, USA, 2007.
15. Madigan, M.T.; Martinko, J.M.; Parker, J. *Brock Biology of Microorganisms*, 10th ed.; Pearson: New York, NY, USA, 2003.
16. Mitchell, J.K.; Santamarina, J.C. Biological considerations in geotechnical engineering. *J. Geotech. Geoenviron. Eng.* **2005**, *131*, 1222–1233. [CrossRef]
17. Nafisi, A.; Safavizadeh, S.; Montoya, B.M. Influence of microbe and enzyme-induced treatments on cemented sand shear response. *J. Geotech. Geoenviron. Eng.* **2019**, *145*, 06019008. [CrossRef]
18. Khodadadi, T.H.; Kavazanjian, E.; van Paassen, L.; DeJong, J. Bio-grout materials: A review. In Proceedings of the Grouting 2017: Grouting, Drilling, and Verification, Honolulu, HI, USA, 9–12 July 2017; Byle, M.J., Johnsen, L.F., Bruce, D.A., El Mohtar, C.S., Gazzarrini, P., Richards, T.D., Eds.; ASCE: Reston, VA, USA, 2017. GSP 288. pp. 1–12. [CrossRef]
19. Javadi, N.; Khodadadi, H.; Hamdan, N.; Kavazanjian, E. EICP treatment of soil by using urease enzyme extracted from watermelon seeds. In Proceedings of the International Foundation Congress and Equipment Expo 2018, Orlando, FL, USA, 5–10 March 2018; Stuedlein, A.W., Lemnitzer, A., Suleiman, M.T., Eds.; ASCE: Reston, VA, USA, 2018. GSP 296. pp. 115–124. [CrossRef]
20. Dilrukshi, R.A.N.; Kawasaki, S. Effective use of plant-derived urease in the field of geoenvironmental/geotechnical engineering. *J. Civ. Environ. Eng.* **2016**, *6*, 1000207. [CrossRef]
21. Dilrukshi, R.A.N.; Watanabe, J.; Kawasaki, S. Strengthening of sand cemented with calcium phosphate compounds using plant-derived urease. *Int. J. GEOMATE* **2016**, *11*, 2461–2467. [CrossRef]
22. Almajed, A.; Khodadadi Tirkolaei, H.; Kavazanjian, E. Baseline investigation on enzyme-induced calcium carbonate precipitation. *J. Geotech. Geoenviron. Eng.* **2018**, *144*, 04018081. [CrossRef]
23. Yasuhara, H.; Neupane, D.; Hayashi, K.; Okamura, M. Experiments and predictions of physical properties of sand cemented by enzymatically-induced carbonate precipitation. *Soils Found.* **2012**, *52*, 539–549. [CrossRef]
24. Martin, K.K.; Khodadadi, T.H.; Kavazanjian, E. Enzyme-induced carbonate precipitation: Scale-up of bio-cemented soil columns. In Proceedings of the Geo-Congress 2020: Biogeotechnics, Minneapolis, MN, USA, 25–28 February 2020; Kavazanjian, E., Hambleton, J.P., Makhnenko, R., Budge, A.S., Eds.; ASCE: Reston, VA, USA, 2020. GSP 320. pp. 96–103. [CrossRef]
25. Prendergast, L.J.; Gavin, K. A review of bridge scour monitoring techniques. *J. Rock Mech. Geotech. Eng.* **2014**, *6*, 138–149. [CrossRef]
26. Zomorodian, S.M.A.; Soleymani, A.; O'Kelly, B.C. Briefing: Improving erosion resistance of sand using nano-silica additive. *Proc. Inst. Civ. Eng. Ground Improv.* **2019**, *172*, 3–11. [CrossRef]
27. Rabiei, A.; Zomorodian, S.M.A.; O'Kelly, B.C. Reducing hydraulic erosion of surficial sand layer by inoculation of cyanobacteria. *Proc. Inst. Civ. Eng. Ground Improv.* **2022**, *175*, 209–221. [CrossRef]
28. Rabiei, A.; Zomorodian, S.M.A.; O'Kelly, B.C. Reducing the erodibility of sandy soils engineered by cyanobacteria inoculation: A laboratory investigation. *Sustainability* **2023**, *15*, 3811. [CrossRef]
29. Štefanac, Z.; Tomašković, M.; Raković-Tresić, Z. Spectrophotometric method of assaying urease activity. *Anal. Lett.* **1969**, *2*, 197–210. [CrossRef]
30. Moody, L.F. Friction factors for pipe flow. *Trans. ASME* **1944**, *66*, 671–678. [CrossRef]
31. Briaud, J.L.; Govindasamy, A.V.; Shafii, I. Erosion charts for selected geomaterials. *J. Geotech. Geoenviron. Eng.* **2017**, *143*, 04017072. [CrossRef]